J. Membrane Biol. 197, 33–48 (2004)
DOI: 10.1007/s00232-003-0638-7

The Journal of
Membrane
Biology

Architecture of the Alzheimer's AβP Ion Channel Pore

N. Arispe
Department of Anatomy, Physiology and Genetics, and Institute for Molecular Medicine, Uniformed Services University School of Medicine, USUHS, Bethesda, MD, 20814, USA

Received: 8 August 2003/Revised: 19 September 2003

Abstract. We have proposed that the cytotoxic action of Alzheimer's amyloid beta protein might be initiated by the interaction with the neuronal cell membrane, and subsequent formation of toxic ion channels. Consequently, AβP toxicity can be explained on the basis of harmful ion fluxes across AβP channels. The conformation of AβP in membranes is not known. However, several models suggests that a transmembrane annular polymeric structure is responsible for the ion channel properties of the membrane-bound AβP. To identify that portion of the AβP molecule making up the conducting pore we have hypothesized that the region of the AβP sequence in the vicinity of the hypothetical pore might interact with complementary regions in the adjacent AβP subunits. We have further hypothesized that an interaction by a peptide segment would block AβP conductance. To test this hypothesis we synthesized peptides that encompass the histidine dyad (H-H) previously hypothesized to line the pore. We report here that peptides designed to most closely match the proposed pore are, in fact, the most effective at blocking ion currents through the membrane-incorporated AβP channel. As previously shown for Zn^{2+} blockade, peptide blockade is also asymmetric. The results also provide additional evidence for the asymmetric insertion of the AβP molecules into lipid membranes, and give support to the concept that rings of histidines line the entry to one side of the AβP pore.

Key words: Alzheimer's disease — Amyloid-β-peptide — Amyloid beta — AβP ion channels — Blocker peptides — Pore region

Correspondence to: N. Arispe; email: narispe@usuhs.mil

Introduction

In Alzheimer's disease (AD), the main pathological features are localized accumulations of amyloid plaques and neurofibrillary tangles in the brain (Mattson, 1997). A major component of the plaques are beta-amyloid peptides (AβPs) of up to 43 amino acids (Glenner & Wong, 1984; Schmechel et al., 1993; Masters et al., 1995). These peptides are produced from amyloid precursor protein (APP) by the activity of specific enzymes (Haass & Selkoe, 1993; Haass et al., 1992). Although there are many genetic etiologies for AD, the accumulation of AβP in plaques is always observed (Selkoe, 1991, 1994; Scheuner, 1996). It has therefore been hypothesized that AβPs are important neurotoxic principles responsible for neuronal cell death in the development of the disorder (Yankner, Duffy & Kirschner, 1990; Neve al., 1990; Selkoe, 1991; Hardy & Higgins, 1992; Kowall et al., 1992; Maloof et al., 1992; Mattson et al., 1992; Frazer, Suh & Djamgoz, 1997). One of the consequences of the interaction between AβP and neurons is the generation of an increase in the intracellular calcium concentration that could, when large enough, create an imbalance of the calcium homeostasis. This effect has been proposed to mediate neurotoxicity (Mattson et al., 1992). It has also been postulated that calcium influx occurs when AβP directly interacts with components in the lipid bilayer matrix of the plasma membrane. The proposed mechanisms include the direct interaction of AβPs with the membrane components to destabilize the structure of the membrane (Muller et al., 1995; Mason et al., 1996; Avdulov et al., 1997; Lee, 2001), as well as insertion of AβP into the membrane to form a cation-conducting pore (Arispe, Rojas & Pollard, 1993a, b, 1996a; Galdzicki et al., 1994; Kawahara et al., 1997; Rhee, Quist & Lal, 1998; Lin, Zhu & Lal, 1999; Lin, Bhatia & Lal, 2001; Hirakura, Lin & Kagan, 1999; Vargas, Alarcon & Rojas, 2000; Lin & Kagan, 2002).

Such channel activity can be observed in both planar lipid bilayers (Arispe et al., 1993b; Arispe, Pollard & Rojas, 1994, 1996; Mirzabekov et al., 1994; Furukawa, Abe & Akaike, 1994; Rhee et al., 1998; Lin et al., 1999; Hirakura et al., 1999, 2000; Bhatia, Lin & Lal, 2000; Zhu, Lin & Lal, 2000; Lin et al., 2001; Lin & Kagan, 2002), and cultured neurons (Simmons & Schneider, 1993; Galdzicki et al., 1994; Kawahara et al., 1997).

Because of the association of extracellular AβP brain deposits or plaques with AD, considerable effort has focused on determining the solution and solid-state structure of AβP. Most studies describing conformation of AβPs in solution note that stable oligomers of AβP occur prior to the appearance of much larger aggregates. In solution, AβPs adopt mixtures of β-sheet, β-helix and random coil conformations, with relative ratios being strongly influenced by both time and concentration. The conversion of monomeric AβP to fibrillar AβP is a transition from random coil to β-sheet (Pike, Overman & Cotman, 1991; Barrow et al., 1992, Terzi, Holzemann & Seelig, 1995). Unfortunately, the relevance of these data to the conformation of AβP pores in membranes is not clear because of the stratified hydrophilic/hydrophobic environment of the membrane. To approach this question, high-resolution Atomic Force Microscopic (AFM) images of AβP oligomers incorporated into lipid bilayers have been meticulously analyzed and associated with AβP pores (Lin et al., 2001), and theoretical methods have been used to develop models for the ion-channel structure of the membrane-bound AβP (Durell et al., 1994). Because of the suspected large physical size of the AβP channel structures, the theoretical models have been designed as polymers of many membrane-bound AβP subunits, in which the secondary structure of the AβP subunit is subdivided into two α-helices and a β-hairpin structure. Hydrophilic residues of the structure project to the lumen of the pore. Experimental support for some of these theoretical models has come from AFM amplitude mode images of AβP reconstituted in membranes, and from studies of the interaction of Zn^{2+} ions with AβP channels. The polymeric conformation of many membrane-bound AβP subunits has been confirmed by the channel-like oligomeric structures observed in the AFM images of AβP reconstituted in planar lipid bilayers (Lin et al., 2001). The orientation of AβP in the membrane has been deduced to be asymmetric due to the fact that Zn^{2+} preferentially binds and blocks only one side of the channel (Arispe et al., 1996a; Vargas et al., 2000). In many proteins Zn^{2+} binds to histidine residues. Consistently, least-energy calculations for model construction indicate a ring of histidine residues around the entrance of the putative pore (Durell et al., 1994).

On the assumption that amyloid fibrils are responsible for toxicity, attempts have been made to block AβP-AβP interaction with peptides from the primary AβP sequence (Ghanta et al., 1996; Soto et al., 1996; Tjernberg et al., 1996; Wood et al., 1996). Ligand peptides that are homologous to the certain regions of AβP and with the same degree of hydrophobicity, have been found to bind to AβP and to block the interaction between monomers and oligomers, thereby inhibiting the formation of amyloid fibrils (Ghanta et al., 1996; Soto et al., 1996; 1998; Tjernberg et al., 1996; Wood et al., 1996; Poduslo et al., 1999; Soto 1999a, b, 2001; Soto, Saborio & Permanne, 2000). We have used the same strategy to design the peptides that, according to the theoretical models, might interfere with ionic currents through the AβP channels. This strategy has allowed us to test the hypothesis that histidines are located predominantly on the AβP channel pore. We report here that peptides that preserve the His-His motif block AβP channels. We discuss the implications of these results for the architecture of the AβP channels and the regions in the AβP subunits that participate in the makeup of the pore.

Materials and Methods

The methods used here have been previously described (Arispe et al., 1993a, b, 1996a). The AβP channel incorporation into the phospholipid membranes was achieved indirectly by fusion of AβP-carrying proteoliposomes with planar phospholipid bilayers.

Preparation of Proteoliposomes

Liposomes were prepared by hydration of air-dried palmitoyloleoyl phosphatidylserine (10 mg) with 1M potassium aspartate, pH 7.0 (1 ml), followed by water sonication for 5 min. The liposome suspension (50 μl) was mixed with a stock aqueous solution of AβP (1 mg/ml, obtained from Bachem, and from AnaSpec, San Jose, CA), followed by sonication for an additional period of 2 min. An aliquot (5 μl) of the proteoliposome suspension was added to the solution on the cis side of the planar lipid bilayer chamber and stirred. After successful ion-channel incorporation was achieved, proteoliposomes were perfused from the chamber prior to test-peptide addition.

Planar Lipid Bilayer Methodology

Planar lipid bilayers were made as described (Arispe et al., 1993). Briefly, a suspension of palmitoyloleoyl phosphatidylserine and palmitoyloleoyl phosphatidylethanolamine, 1:1, in *n*-decane was prepared. This suspension was applied to an orifice of about 100–120 μm in diameter with a Teflon™ film separating two compartments, 1.2 ml volume each. The ionic solutions in the compartments contained asymmetrical concentrations of CsCl (200_{cis}/50_{trans} mM) and symmetrical 0.5 mM $CaCl_2$ and 5 mM K-HEPES, pH 7. The two ionic compartments were electrically connected via agar bridges and Ag/AgCl-pellet electrodes to the input of a voltage-clamp amplifier. Current was recorded using a patch-clamp amplifier (Axopatch-1D equipped with a low-noise (CV-4B) headstage; Axon Instruments, Foster City, CA), and data were simultaneously stored on a PCM/VCR digital system (Toshiba) with a frequency response in the range from direct current to 25,000 Hz, and on computer disk memory. Off-line analysis of the

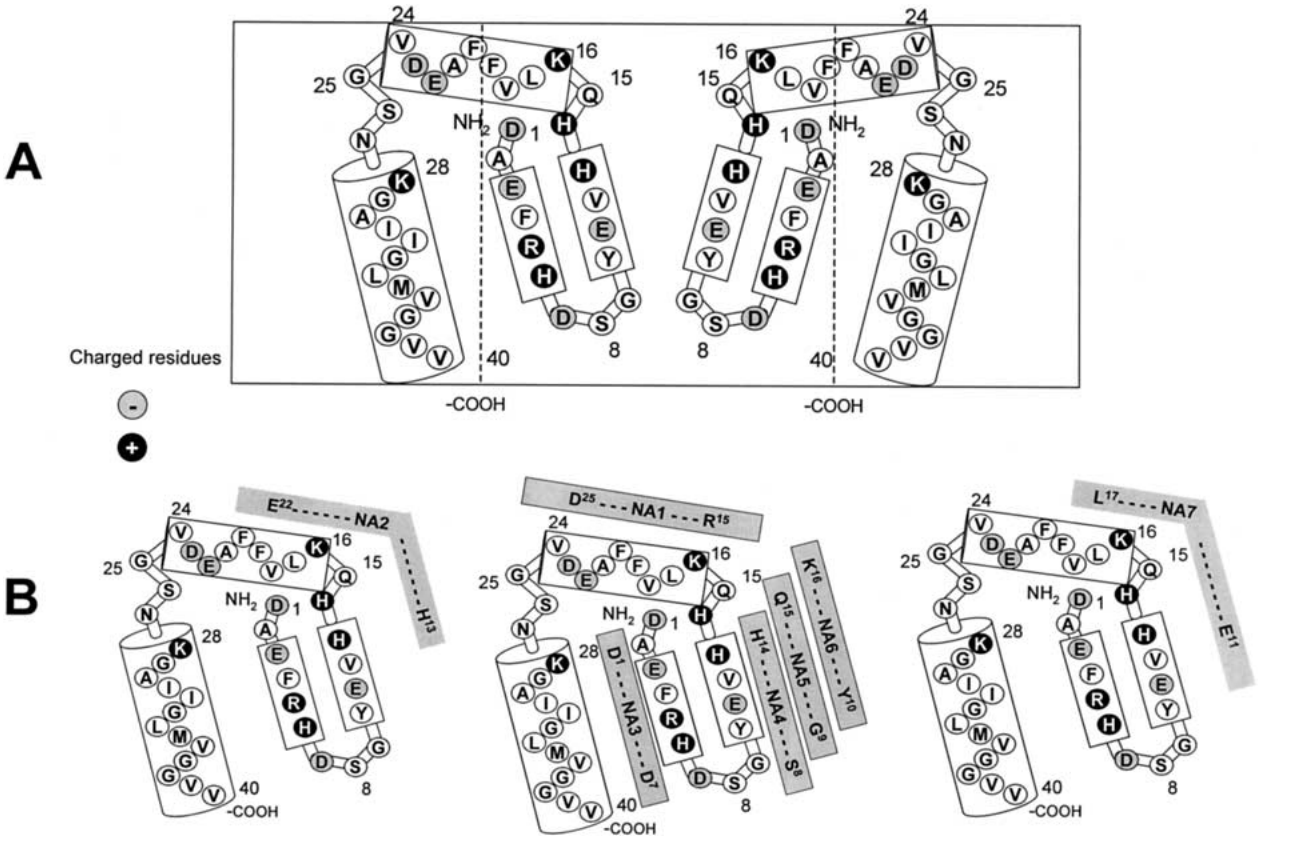

Fig. 1. Theoretical model of a membrane-bound AβP ion channel, modified from Durell et al., 1994. (*A*) Two AβP subunits have been placed in a two-dimensional array in order to illustrate the formation of a hydrophilic pore. (*B*) The seven ligand-binding peptides (gray boxes) have been laid next to the homologous regions of AβP subunits, to illustrate the binding regions relative to the putative pore, and to the central hydrophobic region that harbors the binding sequence required for the polymerization of AβP into amyloid fibrils (Wood et al. 1995, 1996).

channel activity was carried out using the software package Pclamp 6 (Axon Instruments, Foster City, CA).

Peptide Synthesis

We have synthesized eight peptide segments from the AβP sequence. NA1 is made of eleven residues with the following sequence: RDLPFFPVPID. NA2 is made of ten residues with the following sequence HHQKLPFFAE. NA3, NA4, NA4a, NA5, NA6 and NA7 are made of seven residues with the following sequences: DAEFRHD, SGYEVHH, SGGEVHH, GYEVHHQ, YEVHHQK, and EVHHQKL, respectively. These peptides were synthesized in the Biomedical Instrumentation Center at the Uniformed Services University of the Health Sciences, Bethesda, MD, utilizing an Applied Biosystems model 433A peptide synthesizer. The chemistry used to produce the peptides was the HBTU/DIEA activation of Fmoc amino acids. The purity of the peptides was confirmed by HPLC, and an automatic protein sequencer, Applied Biosystems model 476, confirmed the sequence. The amino-acid sequence of the NA1 peptides was constructed as in Soto et al. (1996), with homology similar to the sequence of the AβP regions believed to participate in the polymerization of AβP. As illustrated in Fig. 1, NA3 matches the sequence of the first arm of the β-hairpin structure and NA4, NA4a, NA5, NA6 and NA7 match the regions that line the hypothetical pore of the ion-channel structure of the membrane-bound AβP subunit (Durell et al., 1994). Based on the architecture of the theoretical model for an AβP channel incorporated in a membrane, as shown in Fig. 1*A*, the NA2 and NA7 binding peptides were constructed to interfere with one of the putative mouths of the pore. NA2 and NA7 also interfere with a central hydrophobic region, within the N-terminal domain of AβP, close to Aβ16-20. This region has been reported to be important for the adoption of the correct β-pleated sheet structure of AβP (Wood et al., 1995, 1996), and therefore is a region necessary for AβP polymerization into amyloid fibrils. To test the effect of the peptides on the AβP ion channel, aliquots of 6 μl of peptide stock solutions (1 mg/ml) were added to one side of the chamber, and the electrical activity was monitored. If no effect was observed after a reasonable period of time, the peptide was studied on the other side of the chamber.

Results

Peptides that Match the Sequence of the Proposed AβP Pore Region Affect AβP Channel Conductance

AβP Channel Blockage with NA2 and NA7

The ionic current recorded after the incorporation of AβP (1–40) into planar lipid membranes confirms that AβP (1–40) forms cation-selective channels.

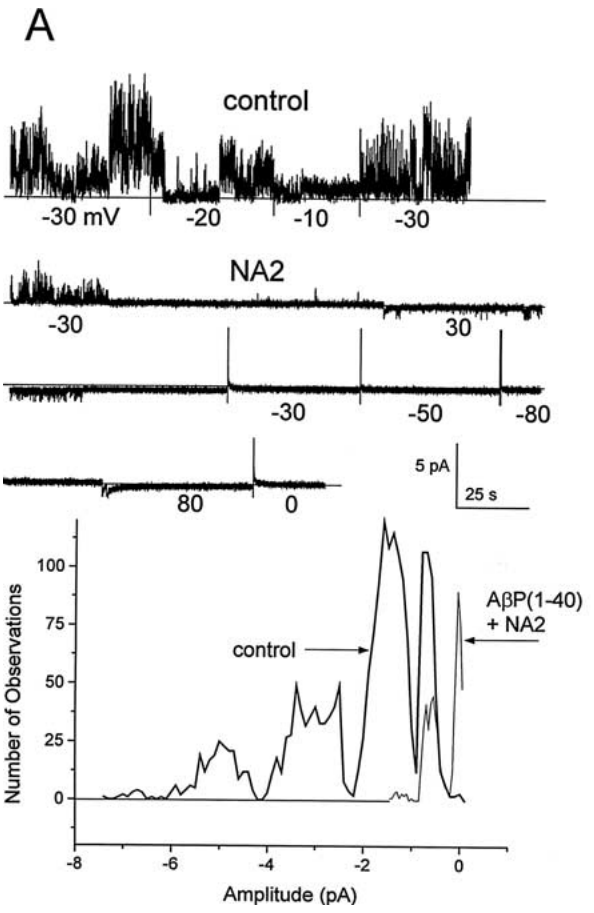

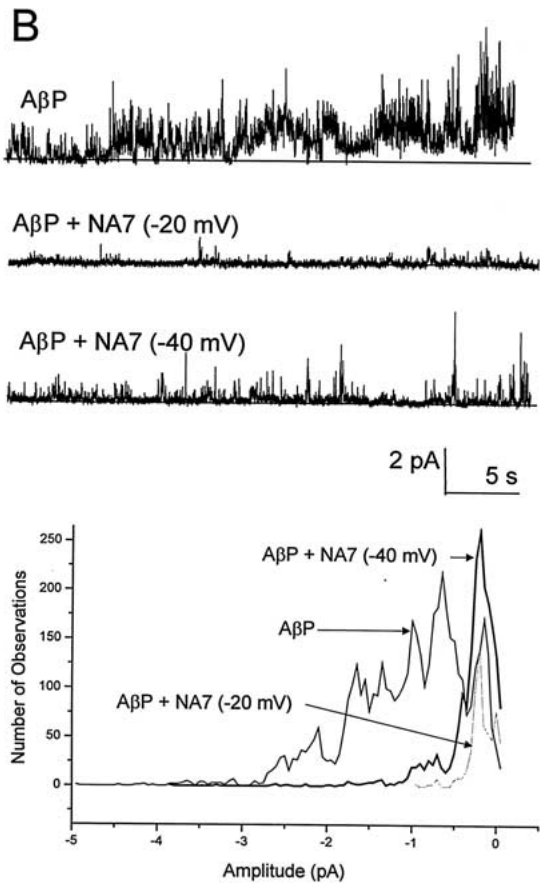

Fig. 2. NA2 and NA7 block the membrane-bound AβP ion channel. (*A*) AβP ion channel electrical activity recorded at different membrane potentials before and after the addition of NA2 (5 μM) to the cis compartment of the experimental chamber. (*B*) AβP ion channel electrical activity recorded before (*control*, 0 mV) and after the addition of NA7 (7 μM), (two lower current recordings). Electrical potential gradients of −20 and −40 mV were imposed on the membrane to enhance the driving force on the ions. The bottom panel displays current-amplitude histograms of the channel activity in the current traces shown above.

Figure 2 illustrates two examples of AβP (1–40) channel activity recorded from planar lipid bilayers separating asymmetrical CsCl solutions (50 mM CsCl on the cis side and 200 mM $CsCl_2$ on the trans side). When AβP-carrying proteoliposomes fuse with the bilayer, and incorporation of AβP (1–40) molecules occurs, current jumps indicate the formation of a cationic channel across the membrane. Current records in the upper panels of Fig. 2*A* and *B* depict channel events. Although no transmembrane potential was imposed in the experiment displayed in Fig. 2*B*, discrete jumps of current to different levels were observed throughout. Upward deflections of current traces represent a flow of Cs^+ from the trans to the cis side. The existing trans/cis Cs^+ concentration gradient is the driving force. Incomplete closures suggest that the AβP (1–40) channel operates between multiple conductance levels, as it has been described elsewhere (Arispe et al., 1993a, b). After the ionic current through the incorporated AβP channels appeared stable for several minutes, we studied the effect of binding of NA2 and NA7 to the AβP molecules on the AβP ion channel activity. The records in Fig. 2*A* illustrate the AβP ion channel electrical activity taken at various membrane potentials (−10, −20 and −30 mV) before (control) and after the addition of NA2 (5 μM) to the cis compartment. Seven minutes after the addition of the peptide, the peaks of current observed in the control records disappeared, indicating that the AβP ion channel electrical activity has been blocked by NA2. Higher membrane potentials of both polarities (30, 50 and 80 mV) were ineffective in restoring the current observed before the blockage. An amplitude histogram of the current events of the channel activity recorded at −30 mV shows five main current peaks of 0.7, 1.5, 2.5, 3.5, and 4.9 pA in the control conditions. After the addition of NA2, only current events of the smallest amplitude, ca. 0.7 pA, were observed just before the electrical recording became silent. The top record in Fig. 2*B* illustrates the AβP ion channel electrical activity taken before the addition of the peptide NA7. No transmembrane potential was imposed in this condition. However, discrete jumps of current to

different levels were observed throughout. After the addition of NA7 (7 μM) to the cis compartment, the current activity vanished (*not shown*). Increasing the driving force for the ions by the application of membrane potential (−20 and −40 mV) reinstated some current activity. However, it never reached the level of the activity in the control record. A current-amplitude histogram to evaluate the most frequent current events of the activity displayed in the control at 0 mV, and at −20 and −40 mV in the presence of NA7 is shown at the bottom of the panel. At 0 mV, the AβP channel showed seven main peaks of current of 0.15, 0.65, 1.0, 1.35, 1.65, 2.1 and 2.5 pA. In the presence of NA7 most of these peaks of current disappeared and the channel remained blocked, even after higher membrane potentials. After the AβP channel was blocked, the peptides NA2 and NA7 were removed from the experimental chamber by rinsing the compartments with peptide-free solutions. However, this maneuver failed to reinstate the ionic currents (*not shown*). Since NA2 and NA7 are expected to interact with the adjoining, complementary $A\beta P_{11-22}$ region, the results support the theoretical model that positions the pore within this region of the AβP ion channel (Durell et al., 1994).

Blocking the AβP Channel with NA5 and NA6

AβP ion channel electrical activity also became electrically silent in the presence of either NA5 or NA6. The experiments displayed in Fig. 3 show the gradual disappearance of the ionic current from two AβP channels incorporated in lipid bilayers at zero membrane potential, after the addition of NA5 (Fig. 3*A*) and NA6 (Fig. 3*B*) peptides (7 μM) to the cis compartment. In both cases, the current level eventually declined to the basal level after 4 minutes and 3 minutes, respectively. The example in Fig. 3*B* shows that before the channel was completely blocked, the binding of NA6 to AβP switched the conformation of the channel to be open at two defined and stable conductance levels with current of amplitudes of 1.2 and 1.6 pA. Upon removal of the blocking peptide from the chamber by replacing the bathing solution 6 times with peptide-free solution, the AβP channel activity totally recovered. In the study with NA5, the current-amplitude histogram of the initial condition shows an AβP channel with most frequent current peaks of 0.4, 1.6, 3.1 and 5.3 pA. They are completely recovered after NA5 is removed. In the study with NA6, the current-amplitude histogram of the control condition shows current peaks of 0.4, 1.0, 1.9 and 3.1 pA. Upon interaction of NA6 and the AβP channel, the most frequent peak values changed to 0.4, 1.2 and 1.6 pA. After 3 minutes in the presence of NA6 almost all current events had disappeared. When NA6 was removed, the histogram reveals an increase in the number of observations corresponding to current peaks at 0.4, 1.2 and 1.6 pA. This indicates that the AβP channels have returned to the last conductance conformations they had upon interacting with NA6, and before it was fully blocked.

Blocking the AβP Channel with NA4 and NA4a

These two heptamer peptides possess similar sequences to a region in the second arm of the β-hairpin ($A\beta P_{8-14}$). This region is believed to line the pore of the ion-channel structure of the theoretical model for a membrane-bound AβP channel (Durell et al., 1994). NA4 and NA4a are similar heptamers: the tyrosine in position 10 of the AβP molecule is copied in NA4 but is substituted by a glycine residue in NA4a. Both peptides were found to be excellent AβP ion-channel blockers, as can be seen in the experiments depicted in Fig. 4. The current records in Fig. 4*A* show the activity from an AβP channel incorporated in a lipid bilayer that was maintained at zero membrane potential. Addition of NA4 (7 μM) to the cis compartment totally eliminates the ionic current and the records become electrically silent. As shown in the experiment displayed in Fig. 4*B*, the peptide NA4a is similarly effective in blocking AβP ion channels. NA4a was added after the AβP channel was incorporated into a lipid bilayer, and maintained at a membrane potential of −20 mV. The ionic current was promptly blocked in the presence of NA4a, and the current activity disappeared from the records (*not shown*). The pattern of channel activity in the control (two upper records of this panel) could not be recovered even after increasing the driving force on the ions by changing the membrane potential to −40 and to −80 mV. The current-amplitude histogram corresponding to this experiment is shown in Fig. 4*D*. At −20 mV the control current records showed four main current peaks at 0.5, 1, 1.9 and 3 pA. 15 seconds after the addition of NA4a, only small current peaks at about 0.3 pA could be recorded. They are absent in the record taken after 3 minutes at a higher (−80 mV) membrane potential.

AβP ion channels are multiconductance channels, and occasionally incorporate into lipid bilayers in conformations that display an almost permanent open conductance state (Arispe et al., 1993, 1994). The blocking effect of NA4 was tested in an AβP channel incorporated with this configuration into a lipid bilayer separating an asymmetric CsCl solution ($200_{cis}/50_{trans}$ mM CsCl). Figure 4*C* shows the behavior of the channel upon the application of different membrane potentials (control). The channel activity behaves almost linearly. A single conductance level of 153 pS is found with infrequent closing events observed at positive membrane potentials. A measurable ion current (2.1 pA) is observed at zero membrane potential, which is generated by ions moving from cis to trans compartments, down the

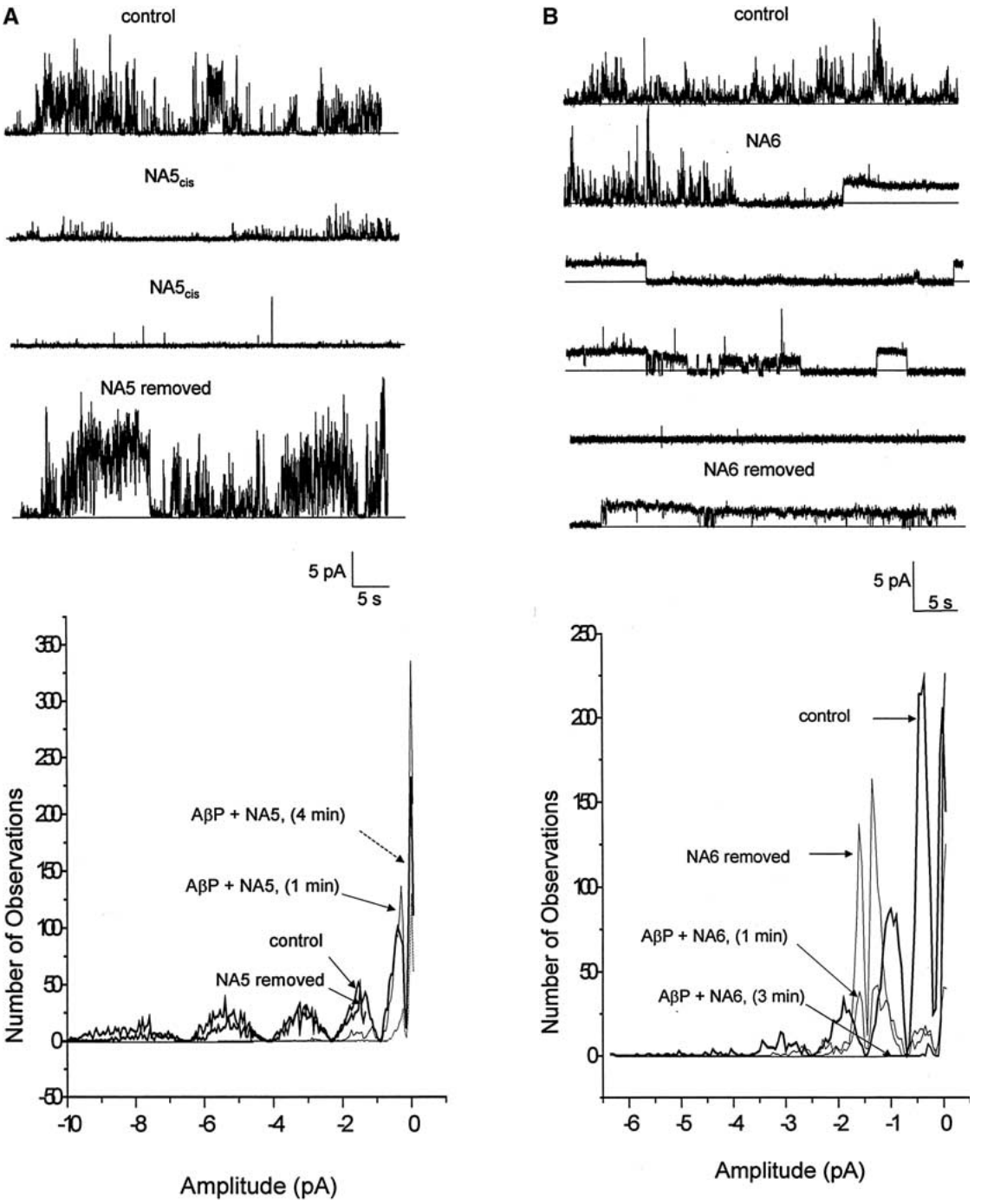

Fig. 3. NA5 and NA6 reversibly block the membrane-bound AβP ion channel. Electrical activities across a lipid bilayer with an incorporated AβP ion channel, recorded before (*control*), during the presence of NA5 (*A*) and NA6 (*B*) peptides (7 μM), and after the peptides were removed from the experimental chamber. During the recordings the membrane potential was maintained at zero level, so the ion fluxes were driven by the existing ionic gradient across the membrane ($200_{cis}/50_{trans}$ mM CsCl). The bottom panel displays current-amplitude histograms of the channel activity in the current traces shown above.

electrochemical gradient. Addition of NA4 (7 μM) to the solution in the trans side of the bilayer generates an increase in the frequency of closing events at positive membrane potentials, which eventually leads to full closing of the channel, as shown in the current record in Fig. 4*Cb*, *1* and *2*. Removing the membrane potential causes the channel to reopen with variable delays, as shown in the two examples in the records in Fig. 4*Cb*, *2* and *3*. Addition of NA4 (7 μM) to the cis side of the bilayer leads to total blockage of currents generated by ions moving from the cis to the trans compartment, as shown in the

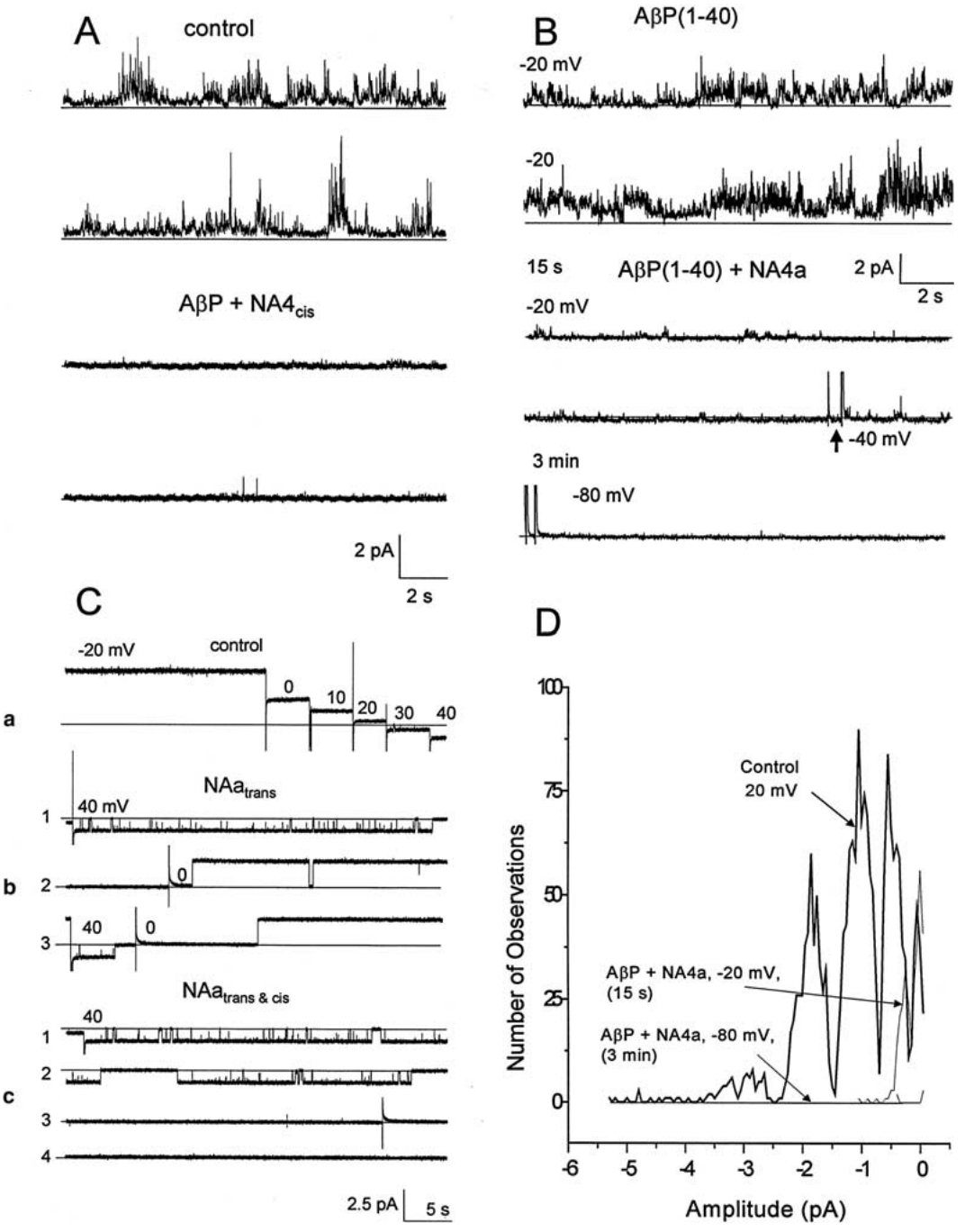

Fig. 4. NA4 and NA4a irreversibly block the membrane-bound AβP ion channel. Electrical activities across lipid bilayers with incorporated AβP ion channels, recorded before (*control*), and in the presence of NA4 (panels *A* and *C*) and NA4a, (panel *B*) peptides (7 μM). The membrane potential in the experiment in *A* was maintained at zero level. In the experiments shown in *B* and *C*, the membrane potential was as indicated. (*D*) Current-amplitude histogram of the channel activity in the current traces shown in panel *B*.

current records displayed in Fig. 4*Cc*, *3* and *4*. In this experiment, NA4 more rapidly blocks the AβP channel when added to the cis side. The efficiency of the blockage by NA4 also depends on whether it has been added at the side from which most of the ions were moving.

We also found that NA4 and NA4a affect AβP ion channels irreversibly. The blockage of the ion-current flux observed after the peptides have been added to the solutions bathing the membrane-bound AβP channel could not be removed by replacing the solutions in the chamber with peptide-free solution or

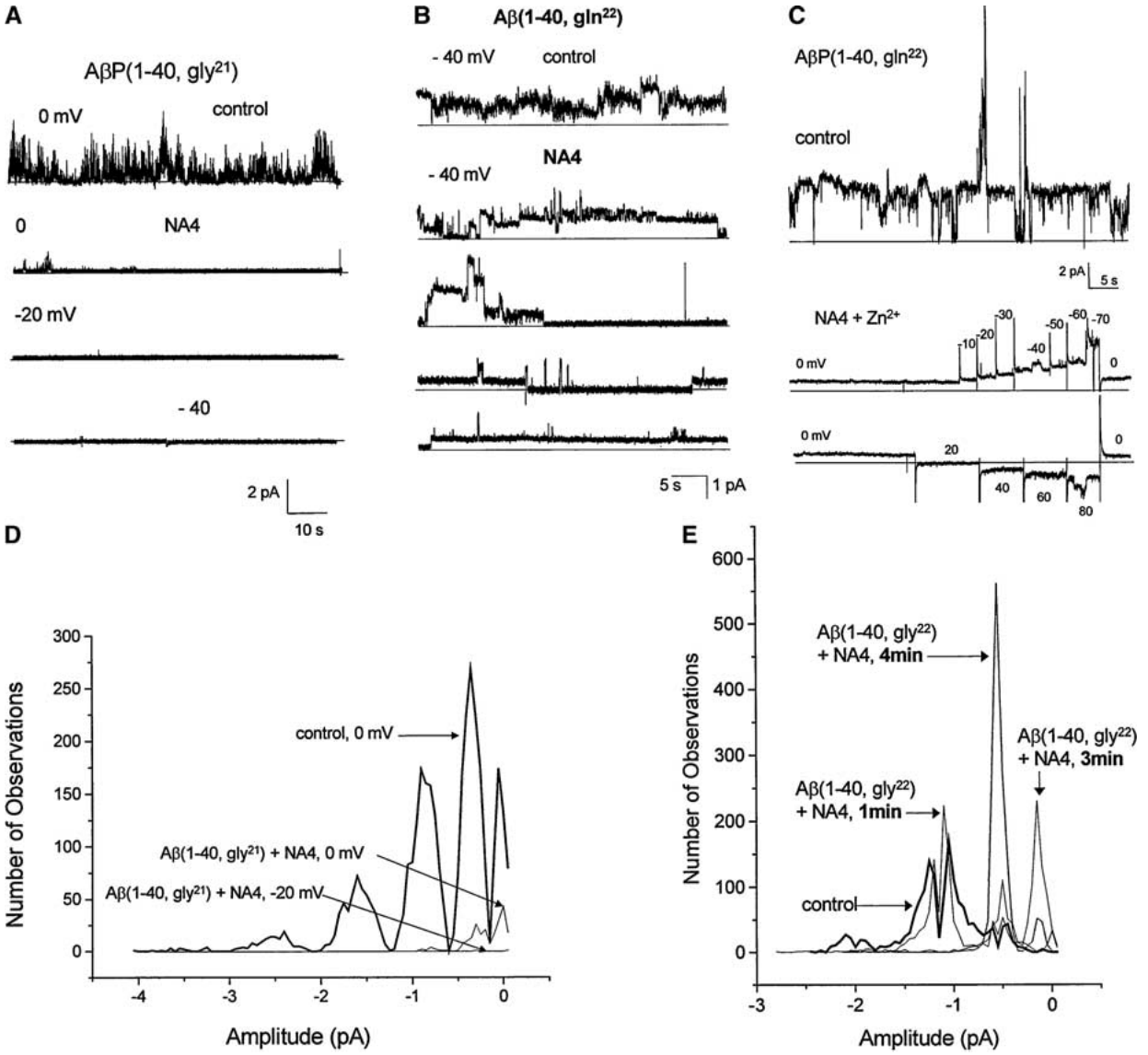

Fig. 5. Effect of the interaction of the peptide NA4 with the "dutch variants" AβP($1–40_{gly21}$) and AβP($1–40_{gln22}$). Discrete jumps of current to different levels indicate the multi-conductance nature of the mutant AβP ion channels. Addition of NA4 (7 μM) results in total elimination of the AβP($1–40_{gly21}$) channel activity, panel *A*, and generates prolonged close events and reduction of the channel activity of AβP($1–40_{gln22}$), panel *B*. The blockage produced by NA4 and Zn^{2+} (500 μM) on AβP($1–40_{gln22}$), could not be removed by the application of larger membrane potentials, panel *C*. The current-amplitude histograms *D* and *E* at the bottom of the figure display the channel activity from the current traces shown in *A* and *B*, respectively.

by changes in the magnitude and polarity of the membrane potential (*not shown*).

"Dutch Variants" AβP Channel Conductance is Affected by the Peptide NA4

We also tested the effect of the interaction of the peptide NA4 with the "Dutch variants" AβPs in planar lipid bilayers. These mutant AβPs are known to be responsible for a form of early onset familial AD. In the "Dutch variants" AβPs there are mutations in either position 21 or 22 within a central hydrophobic region. This region is believed to harbor a binding sequence required for the polymerization of AβP into amyloid fibrils (Wood et al., 1995, 1996). Proteoliposomes containing AβP with mutations at either position 21, AβP($1–40_{gly21}$), or at position 22, AβP($1–40_{gln22}$), were added to the cis compartment of the planar lipid bilayer chamber and allowed to fuse to the membrane. Figure 5 illustrates the electrical activity recorded from membranes separating asymmetrical CsCl solutions (50 mM CsCl on the cis side and 200 mM $CsCl_2$ on the trans side), after the AβP channels were incorporated. The upward-going ionic current in the absence of membrane potential, shown in the upper records

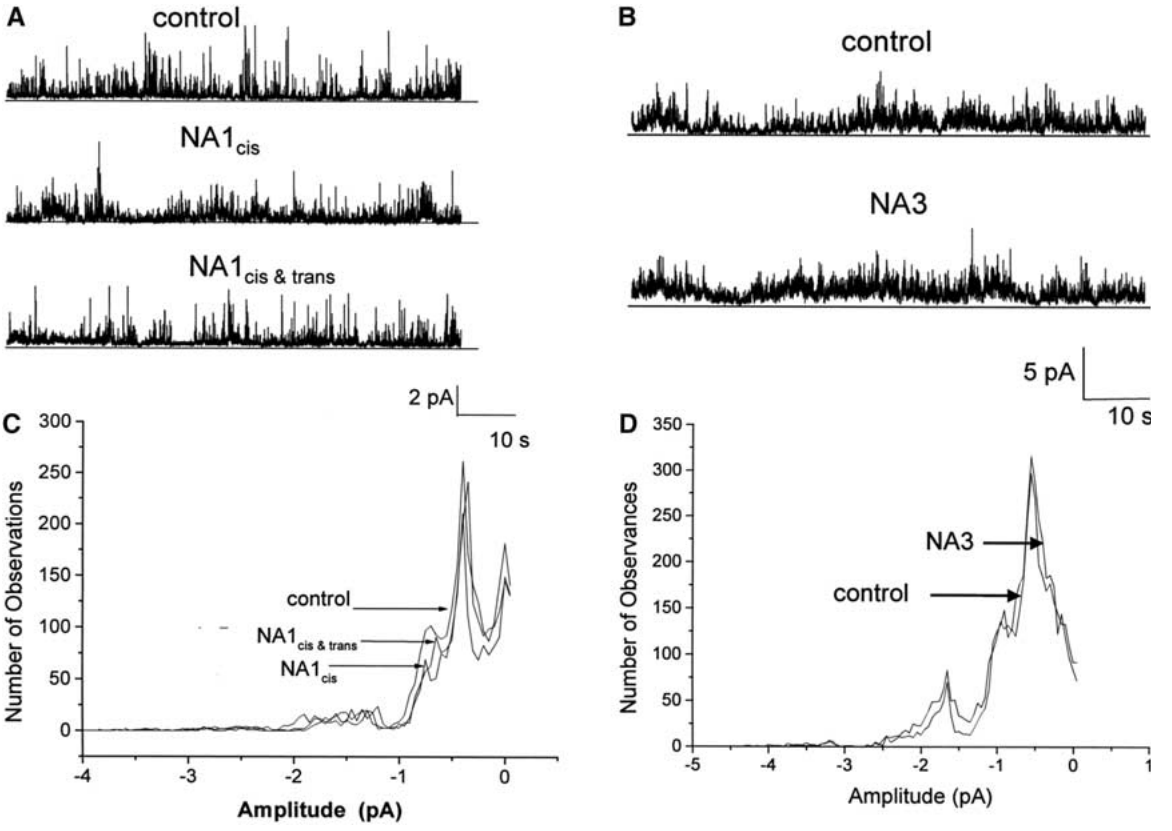

Fig. 6. AβP channel conductance is not affected by the peptides NA1 and NA3. AβP ion channel electrical activity taken before (*control*) and 10 minutes after the addition of NA1 (15 μM) and NA3 (24 μM), *A* and *B*, respectively. No change in the general pattern of the AβP ion channel activity is detected. The amplitude histograms (*C*, *D*) analyze the current events during two minutes of continuous recording, before and after the incorporated AβP channels have been exposed to NA1 and NA3.

of Fig. 5*A* and *C*, confirms that the "Dutch variants" AβPs form cation-selective channels of multi-conductance nature. The amplitude histograms in Fig. 5*D* and *E* show that the discrete jumps of current in the control records gathered at mainly four distinct levels of 0.3, 0.8, 1.6 and 2.4 pA for AβP(1–40_{gly21}), and 0.45, 1.1, 1.3 and 2.1 pA for AβP(1–40_{gln22}). The interaction of NA4 (7 μM) with AβP(1–40_{gly21}) reduced the channel activity almost immediately to current events of 0.3 pA. Soon thereafter the recording became electrically silent. The current events could not be recovered by increasing the membrane potential to −20 mV (Fig. 5*D*). The interaction of NA4 (7 μM) with AβP(1–40_{gln22}), modified the multi-level pattern of current activity observed in control (Fig. 5*B*) to prolonged open levels of 0.45, 1.1 and 1.3 pA; soon thereafter blockade occurred, resulting in current fluctuations between a closed and a small 0.45 pA open state.

The records displayed in Fig. 5*C* illustrate the blockage of an AβP(1–40_{gln22}) channel produced by NA4 (7 μM) with the assistance of zinc (500 μM), a nonspecific AβP blocker. The activity of a large 255 pS AβP channel, with uniform open events of about 5 pA at zero mV membrane potential, was reduced to a very small level characterized by a constant leak current of 0.5 pA. The blockage was so strong that it could not be removed by the application of membrane potentials up to 80 mV.

AβP Channel Conductance Is not Affected by the Peptides NA1 and NA3

We found that addition of either NA1 or NA3 to membrane-bound AβP has no effect on the ion channel activity. NA1 peptide was constructed with homology similar to the sequence of the AβP regions believed to participate in the polymerization of AβP (Soto et al., 1996). The NA3 matches the sequence of the first arm of the β-hairpin structure of the ion channel structure of the membrane-bound AβP subunit (Durell et al., 1994). The current records in Fig. 6 depict the electrical activity of two AβP ion channels treated with the peptides NA1 and NA3. The left panel shows the results of an experiment where NA1 (15 μM) was first added to the cis compartment. Ten minutes later an equal amount was added to the trans compartment. The right

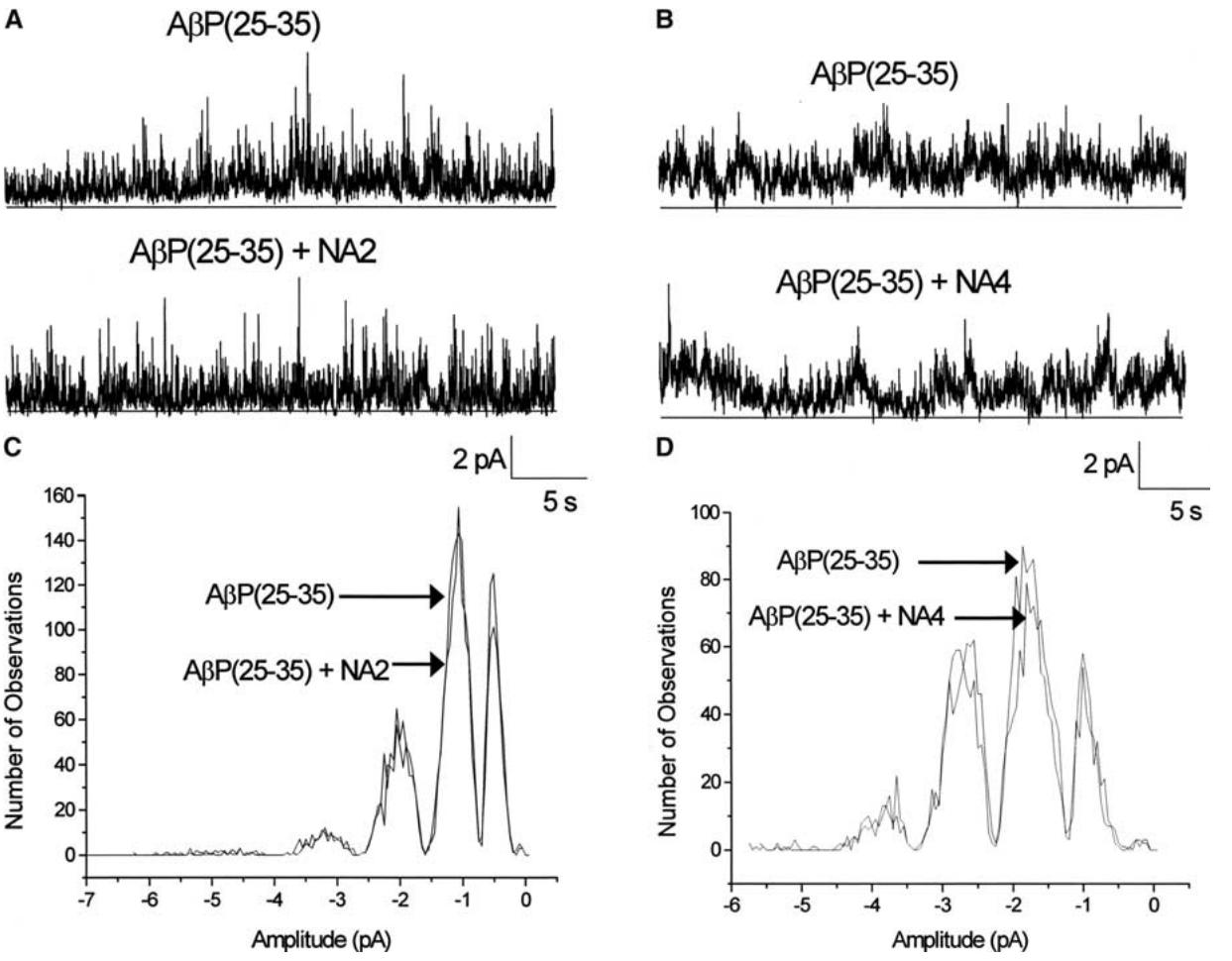

Fig. 7. AβP(25–35) channel conductance is not affected by the peptides NA2 and NA4. AβP(25–35) ion channel electrical activity taken before (*control*) and 20 minutes after the addition of NA2 (14 μM) and NA4 (14 μM), *A* and *B*, respectively, to both the cis and the trans compartments of the experimental chamber. No change in the general pattern of the AβP ion channel activity is detected. The amplitude histograms *C* and *D* analyze the current events during two minutes of continuous recording, before and after the incorporated AβP channels have been exposed to NA2 and NA4.

panel shows the results of an experiment where NA3 (24 μM) was simultaneously added to the cis and the trans compartments. No change in the general pattern of the AβP ion-channel activity was noticed in current records taken 10 and 20 minutes later. The bottom panels show amplitude histograms of the current events during two minutes of continuous recording, before and 20 minutes after the incorporated AβP channels have been exposed to NA1 and NA3. The histograms reveal no difference in either the frequency or amplitude of the current events originating from the channels in control and after peptide treatment. Because the peptide NA1 is expected to bind specifically to the central hydrophobic region of the AβP molecule, the results show that once the AβP ion channel is formed and inserted into the membrane, NA1 binding to this region does not interfere with the AβP ion channel properties.

AβP(1–40) Channel Blockers NA2 and NA4 Do not Affect AβP(25–35) Channel Conductance

To examine the peptides' specific binding to the homologous regions on the AβP molecule, we study the effect of NA2 and NA4, which we found to be effective AβP(1–40) channel blockers, on the current activity from AβP(25–35) channels. The AβP fragment AβP(25–35) has been shown to form ion channels when incorporated in planar lipid bilayers (Mirzabekov et al., 1994, Lin & Kagan, 2002). Figure 7 displays 40-second records of electrical activity of two AβP(25–35) ion channels before and 20 minutes after the addition to the cis and the trans compartments of NA2 (14 μM), left panel, and NA4 (14 μM), right panel. NA2 and NA4, which are homologous to AβP(13–22) and AβP(8–14) respectively, do not change the general pattern of the AβP(25–35) ion-

channel activity. The histograms shown at the bottom of Fig. 7 reveal no difference in either the frequency or amplitude of the current events originating from the channels in control and after peptide treatment.

Discussion

We show here that peptide segments chosen from regions around the putative mouth of the polymeric membrane-bound AβP-channel model effectively affect the channel activity in planar lipid bilayers. Some of the peptides were chosen to include a histidine dyad (H-H), which we have previously modeled to be at the mouth of the pore. The active peptides blocked asymmetrically, as previously demonstrated for Zn^{2+} (Arispe et al., 1996a), and could not be reversed by voltage pulses as high as 80 mV. The results provide additional evidence for the asymmetric insertion of the AβP molecules into lipid membranes and support the prediction for the location of the mouth of the AβP channel in the hypothetical structure for membrane-bound AβP channels.

Spontaneous Transition between Conductance States Characterizes the Kinetics of AβP Channels

Previously we found and described cationic currents from planar lipid bilayers that had been exposed to solutions containing AβP (Arispe et al., 1993b,c, 1994, 1996a). These findings have been corroborated in numerous subsequent publications (Rhee et al., 1998; Lin et al., 1999; Hirakura et al., 1999, 2000; Bhatia et al., 2000; Zhu et al., 2000; Lin et al., 2001; Lin & Kagan, 2002), and the insertion of AβP molecules into the lipid membranes was shown (Vargas et al., 2000; Lee, 2001). However, the capacity of AβP to selectively permit cationic currents across membranes requires that AβP units not only insert but also additionally incorporate in a conformation appropriate to form stable ion channels. The stability of the incorporation of the channels in the membrane is confirmed by the fact that the channel activity can be recorded for extended periods of time. However, stable AβP channels incorporated in planar lipid bilayers may easily undergo conformational changes as expressed by their multi-conductance behavior. We observed in the current recordings and in the current histograms shown in Fig. 3 and Fig. 5 that the binding of NA6 and NA4 to AβP, before the ionic currents are blocked, induced a conformational change that generated new current levels. To analyze the effect of the peptide binding to AβP channels, we considered that analyzing the frequency of the different conductance levels that the channels present for a reasonable period of the life time of the channel, provides a reasonable quantification and might be used to reveal any alteration generated by the peptides on this pattern. We have previously described the irregular pattern of channel events that is a distinctive feature common to AβP channels and to other similar ion channel-forming proteins (Arispe et al., 1993a, b; 1996a, b). The results shown here extend this description to the novel report that "Dutch variants" AβPs also form cation-selective channels of multiconductance nature. Multiple short-duration transitions between closed and different open conformations characterize the electrical activity of these channels. The channel activity that is characterized by long-duration openings with specifically defined mono-conductance is not the general rule for AβP channels, and it is observed only occasionally. Due to the spontaneous transition between conductance states the typical parameters that characterize the kinetics of classical ion channels cannot be utilized to analyze these cases.

The Durell et al. Models for a Membrane-bound AβP Ion Channel

Very little information is available about the conformation of the AβP pore in the stratified hydrophilic/hydrophobic environment of lipid membranes. Thus far we know from asymmetric Zn^{2+}-AβP interactions (Arispe et al., 1996a), and from recordings of displacement currents in response to sudden changes of the potential from membranes containing AβP-bound molecules, that the insertion of AβP into lipid membranes is highly polarized (Vargas et al., 2000). We also know that AβP incorporates into planar lipid bilayers in the form of doughnut-shaped structures protruding out of the membrane surface, with a centralized pore-like depression presumably representing individual channels (Lin et al., 2001). But with regard to the ion-channel structure of the membrane-bound AβP subunit, only theoretical models have been proposed (Durell et al., 1994). These modeling studies of the AβP ion channel have been interpreted in terms of a least-energy, highly probable, asymmetric, polymeric, transmembrane structure. To test this hypothesis experimentally, we have constructed a set of peptides designed to overlap with the predicted pore domain. We hypothesized that those peptides that most closely corresponded to the pore might affect AβP channel most efficiently. The peptides chosen for our experiments are summarized in Figs. 1 and 7. We performed tests of the aggregation and bilayer interaction of the seven peptides by studying the induction of liposome aggregation by the peptides. The liposome aggregation assay has been extensively used in the past to study protein-lipid interaction in a variety of proteins that are known to self-associate to form oligomers (Blackwood & Ernst, 1990; de la Fuente & Parra, 1995; Lee & Pollard, 1997; Arispe, Doh & DeMaio, 2002). The results of these tests were nega-

tive, suggesting that the peptides do not interact with the bilayer and do not self-aggregate. Certain ones of these peptides (*viz*., NA2, NA4, NA4a, NA5, NA6 and NA7) clearly interact to some extent with the AβP channel to affect its ionic conductance. As shown in Figs. 2–4, NA2, NA4, NA4a, and NA7 establish tighter molecular interaction with the channel, as manifest by their irreversible block of the conductance. By contrast, blocks by NA5 and NA6 were reversible. As shown in Fig. 7, the interaction of NA2 and NA4 with the AβP channel is also selective since these peptides do not affect the activity of the AβP(25–35) channel, which displays different residue sequence. When the addition of the test peptide led to the total elimination of the AβP channel activity, as it was the case for NA2 and NA4, the channel activity abruptly disappeared in an all-or-none fashion. Attempts to construct a dose/response curve for the peptides were unsuccessful since an abrupt cessation of activity occurred randomly and at variable times. Such behavior is expected for a single stop-cork type of interaction. Therefore, we report in this paper that peptides designed to most closely match the pore are, in fact, the most effective at altering ion currents through the membrane-incorporated AβP channel. We conclude that the "most probable" model predicted by Durell et al., 1994, may correspond closely to the conformation that AβP actually assumes in membranes. A more systematic study to describe the characteristics of the blockage of the AβP channels by some of the peptides will have to be pursued.

The ion-channel activity analyzed in this work was obtained from the incorporation of AβP(1–40) in lipid bilayers. Nevertheless, we expect that the conclusions from the effect of the peptide segments on the AβP(1–40)-channel activity can also be extended to AβP(1–42) channels. The longer peptide AβP(1–42) has two additional residues at the carboxyl terminal but the amino-acid sequence at the suggested domain of the pore is the same for both AβPs. Compared to AβP(1–40), AβP(1–42) has different lipid affinity and self-aggregation properties (Burdick et al., 1992; Pike et al., 1995; Arispe, 2001), but it has been reported that both AβPs form ion channels in lipid bilayers with similar conductance and ionic current activity (Arispe et al., 1994; Rhee et al., 1998; Hirakura et al., 1999). We therefore anticipate that the interaction with the AβP(1–42) molecules of those peptide segments that mimic the domain of the pore generates the same effect on the channel properties as the one that we observed on the AβP(1–40) channel. It has not been reported that the insertion of AβP(1–40) and AβP(1–42) in lipid membranes occurs in the same channel-like structure, but in support of our prediction, preliminary experiments have shown that the blocker peptides NA2 and NA4 are equally effective in preventing the neurotoxicity of AβP(1–40) and AβP(1–42) on PC12 cells (Arispe & Doh, 2003).

Peptides Affecting AβP Channel Activity Are Different from those Reported to Affect AβP Polymerization

The use of peptides to probe AβP function has been employed in the past. Among these studies, several peptides designed to overlap with hydrophobic stretches of AβP have been studied in terms of their ability to block macroscopic amyloid fibril formation (Ghanta et al., 1996; Soto et al., 1996; Tjernberg et al., 1996; Wood et al., 1996). We synthesized one of these peptides, NA1, to test for possible effects on channel function. NA1 overlaps the middle helix that lays parallel to the membrane plane in one of the theoretical models for the AβP ion channel proposed by Durell et al., 1994 (*see* Fig. 1). Despite the confirmed interaction of NA1 with AβP, the lack of effect on the ionic currents from AβP channels already incorporated into lipid bilayer, shown in Fig. 6, disproves any hypothetical participation of this binding region in the operation of the channel. On the other hand, the blocking effect of NA7 on the ionic currents from AβP channels shown in Fig. 2*B*, despite its lack of ability to block AβP aggregation (Tjernberg et al., 1996), clearly separates channel function from binding. The results obtained by the application of the peptide NA4 on channels made by AβP mutants, as shown in Fig. 5, further confirm this assertion. The ionic current-blocking interaction of the peptide NA4, that was observed on wild-type AβP channels (Fig. 4), is still effective when tried on the "Dutch variants" AβPs channels (Fig. 6). The mutations in these AβP variants at positions 21 or 22 fall within the central hydrophobic region in the middle helix, which does not form part of the predicted pore sequence. Therefore, these data indicate that AβP channel function and AβP fibrillogenesis are independent functions of each other. Fibrils have been considered in the past by some investigators to be the toxic principle in amyloid. However, if AβP channel properties, per se, were to contribute to the functional basis of amyloid neurotoxicity, our data would not exclude the fibrils from otherwise bringing the toxic channels to the place where pathology might be engendered.

Evidences for H-H Dyads at the AβP Channel Mouth

The common feature in these active blocker peptides, as outlined in Fig. 8, is that they all possess in their sequence the two histidine residues modeled to line the entry to the AβP pore. By contrast, NA1 and NA3 showed no effect on AβP channel conductance. Although the sequence of NA3 matches the sequence of one of the branches of the hairpin structure that lines the pore, according to the theoretical model, our experiments did not show any effect of the NA3 peptide on the AβP ionic currents. Although hydro-

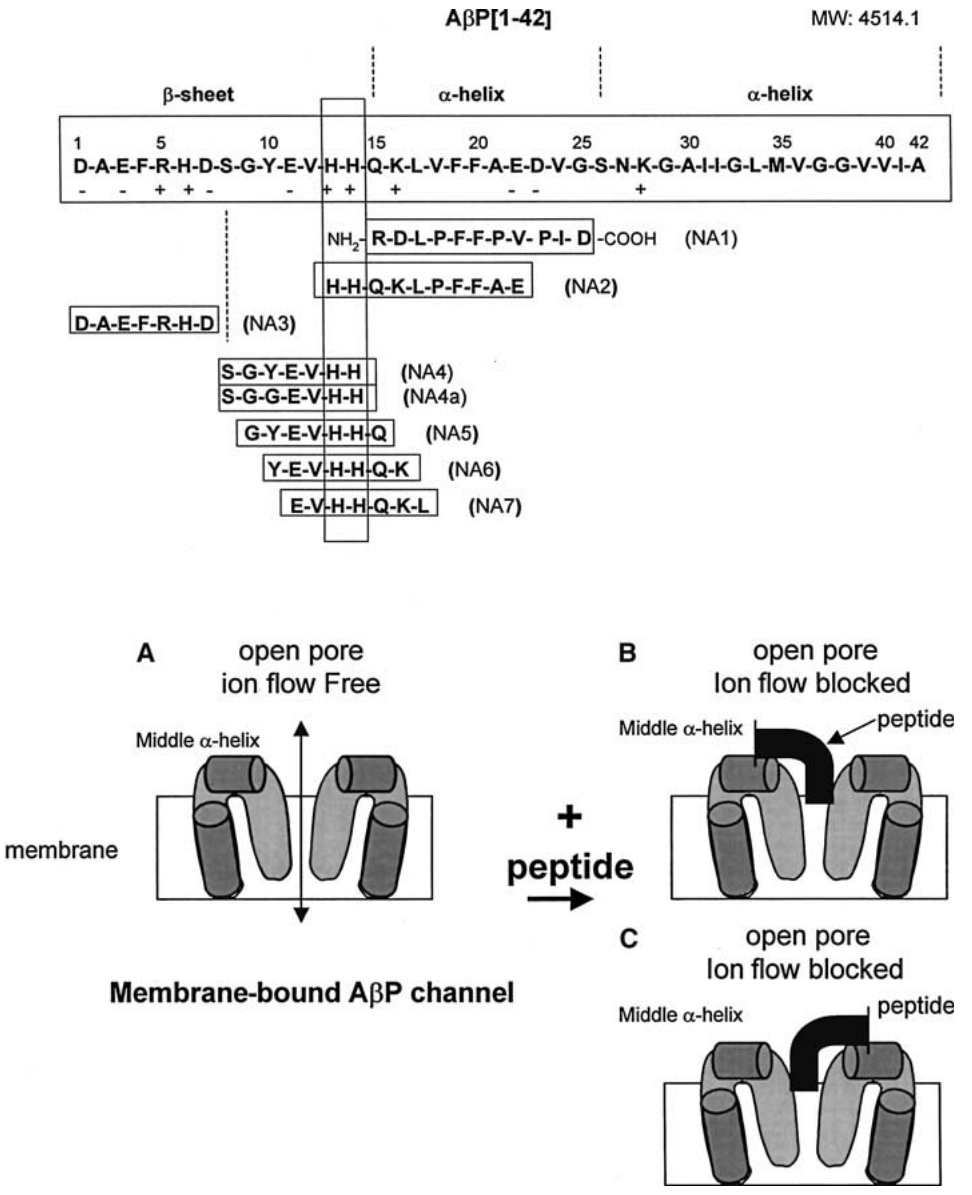

Fig. 8. (*Top*) Amino-acid sequence of the AβP[1–42]. The sequences of the eight test peptides have been boxed and laid out to correspond with the complementary sequence in the AβP molecule. The vertical box illustrates the two common histidine residues in six of the peptides and in the AβP molecule. (*Bottom*) A schematic model for the mechanism of action of a blocker peptide. (*A*) A membrane-bound AβP channel (Durell et al. parallel-type I) in the open state for free flow of ions. (*B* and *C*). A blocker peptide at the mouth of the pore interacts with complementary regions of oppositely located units to block the free flow of ions.

phobicity provides considerable stabilization energy to facilitate peptide-AβP interaction (Tjernberg et al., 1996; Ghanta et al., 1996; Soto et al., 1996), we suspect that to block the ionic current by interaction with AβP channels an additional and more specific interaction is required. We suspect that the required additional binding is provided by the amino acids surrounding the histidines, as well as the two histidine residues that are common in the sequence of the most effective blocker peptides. NA3 matches the sequence of some of the pore lining, but does not possess histidine residues. When AβP subunits form the predicted oligomeric theoretical model of the channel structure in the membrane (Fig. 1*A*), the channel has two rings of histidine residues, His_{13} and His_{14}, encircling one pore entrance. It has been proposed that this conformation enables Zn^{2+} ions to interact asymmetrically with the environment of the conducting pathway and block the AβP channel (Arispe et al., 1996a). A similar line of reasoning can be applied to explain the remarkable blocking effect that we observed upon application of these specific peptides to the AβP channel. Histidines are among the most common amino acids in protein active or binding sites, and they are very common in metal binding sites (e.g., zinc). The imidazole groups on the

side chain of histidine can act as both an acid and a base, i.e., it can both donate and accept protons under some conditions. This means that this amino acid side chain finds its way into considerable use in coordinating binding interactions between proteins. This may be the case for the two rings of histidine residues, His_{13} and His_{14}, encircling one pore entrance of the predicted oligomeric channel structure in the membrane and mediating the binding to the complementary histidine-containing peptides.

Mechanisms for Action of Peptides on AβP Channels

The observed experimental asymmetry of the AβP channel (Fig. 4*C*) in terms of its sensitivity to the blocking peptides is also explained on the basis of the asymmetric localization of the two rings of histidine in the theoretical model for the AβP ion channel. When binding to or near the adjacent histidines is established, the peptide blocks the entrance of the pore and consequently the flow of current through the channel. The model schematized at the bottom of Fig. 8 proposes a mechanism of action in which one of the blocker peptides affects the ionic flow. The model depicts an oligomeric structure of individual AβP molecules that form a membrane-bound AβP channel according to Durell et al.'s parallel type-I model. The NA2 peptide irreversibly blocks AβP channels. In the channel open state for free flow of ions, the blocker peptide finds its way inside the pore of the channel molecule. NA2, which shares the sequence not only with the central hydrophobic region but also with one of the putative mouths of the pore, recognizes and interacts with the middle α-helix of one AβP unit and binds with the histidine region in the opposite AβP unit of the pore. This stable binding by a type of "stop-cork" action alters the free flow of ions through the open pore of the channel. Depending on the number of units that form the oligomeric channel aggregate, additional peptide units can find positions within the pore, enhancing the blocking effect.

In conclusion, the results of our work on the use of peptides that target a specific region of the AβP molecules, provide experimental support to define regions of the AβP sequence that participate in the formation of the pore lining in the membrane-bound AβP ion channel incorporated into planar lipid bilayer. The results also provide additional proof for the asymmetric insertion of the AβP molecules into lipid membranes, and give support to the proposed participation of the ring of histidines at one entrance to the pore of the AβP ion channel. Also derived from the experimental results, we conclude that the architecture of the channel seems to favor one of the three basic models as envisioned by Durell et al., in which the pore is formed by the β-hair pins of the channel. If, as we proposed, there is a connection between AβP ion channels, the death of neurons, and Alzheimer's disease, the definition of the pore of the AβP ion channels may provide a rational basis for design of new therapeutic drugs for Alzheimer's disease.

The author thanks Dr. H.B. Pollard and Dr. D. Mears for invaluable comments and discussion, and Mr. M. Doh for technical assistance. This work was supported by a grant from The Alzheimer's Association of America.

References

Arispe, N. 2001. Control of the interaction of the Alzheimer's AβPs and homologous analogues, with lipid membranes. *Biophys. J.* **80:**135a

Arispe, N.J., Doh, M. 2003. Peptides that block Alzheimer's AβP ion channels protect cells from AβP toxicity. *Biophysical J.* **84:** 53a

Arispe, N., Doh, M., De Maio, A. 2002. Lipid interactions differentiates the constitutive and stress-induced heat shock proteins Hsc70 and Hsp70. *Cell Stress and Chaperones* **7:**330–338

Arispe, N., Pollard, H.B., Rojas, E. 1994. β-amyloid Ca^{2+}-channel hypothesis for neuronal death in Alzheimer disease. *Mol. Cell. Biochem.* **140:**19–125

Arispe, N., Pollard, H.B., Rojas, E. 1996a. Zn^{2+} interaction with Alzheimer amyloid β protein calcium channels. *Proc. Natl. Acad. Sci. USA* **93:**1710–1715

Arispe, N., Rojas, E., Gene, B.R., Wu, L.N.Y., Wuthier, R. 1996b. Similarity in calcium channel activity of annexin V and matrix vesicles in planar lipid bilayers. *Biophys. J.* **71:**1764–1775

Arispe, N., Rojas, E., Pollard, H.B. 1993a. Alzheimer disease amyloid β-protein forms calcium channels in bilayer membranes: blockade by tromethamine and aluminium. *Proc. Natl. Acad. Sci. USA* **90:**567–571

Arispe, N., Rojas, E., Pollard, H.B. 1993b. Giant multilevel cation channels formed by Alzheimer disease amyloid β-protein [AβP-(1–40)] in bilayer membranes. *Proc. Natl. Acad. Sci. USA* **90:**10573–10577

Avdulov, N.A., Cochina, S.V., Igbavboa, U., Warden, C.S., Vassiliev, A.V., Wood, W.G. 1997. Lipid binding to amyloid-β-peptide aggregates. Preferential binding of cholesterol as compared with phosphatidylcholine and fatty acids. *J. Neurochem.* **69:**1746–1752

Barrow, C.J., Yasuda, A., Kenny, P.T.M., Zagorski, M.G. 1992. Solution conformations and aggregational properties of synthetic amyloid β-peptides of Alzheimer's disease. Analysis of circular dichroism spectra. *J. Mol. Biol.* **225:**1075–1093

Bathia, R., Lin, H., Lal, R. 2000. Fresh and globular amyloid-β-protein induces rapid cellular degeneration. A possible implication for calcium-uptake via AβP-channel. *FASEB J.* **14:**1233–1243

Blackwood, R.A., Ernst, J.D. 1990. Characterization of Ca^{2+}-dependent phospholipid binding, vesicle aggregation and membrane fusion by annexins. *Biochem. J.* **266:**195–200

Burdick, D., Soreghan, B., Kwon, M., Kosmoski, J., Knauer, M., Henschen, A., Yates, J., Cotman, C., Glabe, C. 1992. Assembly and aggregation properties of synthetic Alzheimer's A4/beta amyloid peptide analogs. *J. Biol. Chem.* **267:**546–554

de la Fuente, M., Parra, A.V. 1995. Vesicle aggregation by annexin I: role of a secondary membrane binding site. *Biochemistry.* **34:**10393–10399

Durrell, S.R., Guy, H.R., Arispe, N., Rojas, E., Pollard, H.B. 1994. Theoretical models of the ion channel structure of amyloid-β-protein. *Biophys. J.* **67:**2137–2145

Frazer, S.P., Suh, Y.-H., Djamgoz, M.B.A. 1997. Ionic effects of the Alzheimer's disease β-amyloid precursor protein and its metabolic fragments. *Trends Neurosci.* **20:**67–72

Furukawa, K., Abe, Y., Akaike, N. 1994. Amyloid β protein-induced irreversible current in rat cortical neurones. *NeuroReport.* **5:**2016–2018

Galdzicki, Z., Fukuyama, R., Wadhwani, K., Rapoport, S., Ehrenstein, G. 1994. β-amyloid increases choline conductance of PC12 cells: possible mechanism of toxicity in Alzheimer's disease. *Brain Res.* **646:**332–336

Ghanta, J., Shen, C.-L., Kiessling, L.L., Murphy, R.M. 1996. A strategy for designing inhibitors of β-amyloid toxicity. *J. Biol. Chem.* **271:**29525–29528

Glenner, G.G., Wong, C.W. 1984. Alzheimer's Disease: Initial report of the purification and characterization of a novel cerebrovascular amyloid protein. *Biochem. Biophys. Res. Comm.* **120:**885–890

Haass, C., Schlossmacher, M., Hung, A.Y., Vigo-Pelfrey, C., Mellon, A. et al. 1992. Amyloid β-peptide is produced by cultured cells during normal metabolism. *Nature* **359:**322–325

Haass, C., Selkoe, D.J. 1993. Cellular processing of β-amyloid precursor protein and the genesis of amyloid-β-peptide. *Cell* **75:**1039–1042

Hardy, J.A., Higgins, G.A. 1992. Alzheimer's disease: the amyloid cascade hypothesis. *Science* **256:**780–783

Hirakura, Y., Lin, M.C., Kagan, B.L., 1999. Alzheimer amyloid beta peptide 1-42 channels: effect of solvent, pH, and congo red. *J. Neurosci. Res.* **57:**458–460

Hirakura, Y., Yiu, W.W., Yamamoto, A., Kagan, B.L. 2000. Amyloid peptide channels: blockade by zinc and inhibition by Congo red. *Amyloid* **7:**194–199

Kawahara, M., Arispe, N., Kuroda, Y., Rojas, E. 1997. Alzheimer's disease amyloid β-protein forms Zn^{2+}-sensitive cation-selective channels across excited membrane patches from hypothalamic neurons. *Biophysical J.* **73:**67–75

Kowall, N.C., McKee, A.C., Yankner, B.A., Beal, M.F. 1992. In vivo neurotoxicity of beta amyloid [β(1–40)] and thte β(25–35) fragment. *Neurobiol. of Aging* **13:**531–542

Lee, K.Y.C. 2001. Interactions of Alzheimer's amyloid-beta-peptides with lipid membranes. *Biophys. J.* **80:**23a

Lee, G., Pollard, H.B. 1997. Highly sensitive and stable phosphatidylserine liposome aggregation assay for annexins. *Analyt. Biochem.* **252:**160–164

Lin, H., Bhatia, R., Lal, R. 2001. Amyloid protein forms ion channels: implications for Alzheimer's disease pathophysiology. *FASEB J.* **15:**2433–2444

Lin, H., Zhu, Y.J., Lal, R. 1999. Amyloid β-protein (1–40) forms calcium-permeable Zn^{2+} sensitive channels in reconstituted lipid vesicles. *Biochemistry* **38:**11189–11196

Lin, M.C., Kagan, B. 2002. Electrophysiologic properties of channels induced by Aβ25–35 in planar lipid bilayers. *Peptides* **23:**1215–1228

Maloof, A.T. 1992. Effect of beta amyloid peptides on neurons in hippocampal slice cultures. *Neurobiol. of Aging* **13:**543–551

Mason, R.P., Estermyer, J.D., Kelly, J.F., Mason, P.E. 1996. Alzheimer's disease amyloid β peptide 25–35 is localized in the membrane hydrocarbon core: X-ray diffration analysis. *Biochem. Biophys. Res. Comm.* **222:**78–82

Masters, C.L., Simms, G., Weinman, N.A., Multhaup, G., McDonald, B.L., Beyreuther, K. 1985. Amyloid plaque core protein in Alzheimer's disease and Down syndrome. *Proc. Natl Acad. Sci.* USA **82:**4245–4249

Mattson, M.P. 1997. Cellular actions of beta-amyloid precursor protein and its soluble and fibrillogenic derivatives. *Physiol Rev.* **77:**1081–1132

Mattson, M.P., Cheng, B., Davis, D., Bryant, K., Liberberg, I., Rydel, R.E. 1992. β-Amyloid peptides destabilize calcium homeostasis and render human cortical neurons vulnerable to excitoxicity. *J. Neurosci.* **12:**376–389

Mirzabekov, T., Lin, M.C., Yuan, W.L., Marshall, P.J., Carman, M., Tomaselli, K., Lieberburg, I., Kagan, B.L. 1994. Channel formation in planar lipid bilayers by a neurotoxic fragment of the beta-amyloid peptide. *Biochem. Biophys. Res. Commun.* **202:**1142–1148

Muller, W.E., Koch, S., Eckert, A., Hartmann, H., Scheuer, K. 1995. β-amyloid peptide decreases membrane fluidity. *Brain Res.* **674:**133–136

Neve, R.L., Dawes, L.R., Yankner, B.A., Benewitz, L.L., Rodriguez, W., Higgins, G.A. 1990. Genetics and biology of the Alzheimer's amyloid precursor. *Prog. Brain. Res.* **86:**257–267

Pike, C.J., Overman, M.J., Cotman, C.W. 1995. Amino-terminal deletions enhance aggregation of amyloid peptides in vitro. *J. Biol Chem.* **270:**23895–23898

Pike, C.J., Walencewicz, A.J., Glabe, C.G., Cottman, C.W. 1991. In vitro aging of β-amyloid protein causes peptide aggregation and neurotoxicity. *Brain Res.* **563:**311–314

Poduslo, J.F., Curran, G.L., Kumar, A., Frangione, B., Soto, C. 1999. Beta-sheet breaker peptide inhibitor of Alzheimer's amyloidogenesis with increased blood-brain barrier permeability and resistance to proteolytic degradation in plasma. *J. Neurobiol.* **39:**371–382

Rhee, S.K., Quist, A.P., Lal, R. 1998. Amyloid β-protein (1–42) forms calcium-permeable Zn^{2+}-sensitive channels. *J. Biol. Chem* **273:**13379–13382

Scheuner, D., Eckman, C., Jensen, M., Song, X., Citron, M., Suzuki, N., Bird, T.D., Hardy, J., Hutton, M., Kukull, W., Larson, E., Levy-Lahad, E., Vitanen, M., Peskind, E., Poorkaj, P., Schellenberg, G., Tanzi, R., Wasco, W., Lannfelt, L., Selkoe, D., Younkin, S. 1996. Secreted amyloid β-protein similar to that in the senile plaques of Alzheimer's disease is increased in vivo by the presenilin 1 and 2 and APP mutations linked to familial Alzheimer's disease. *Nat. Med.* **2:**864–870

Schmechel, D.E., Saunders, A.M., Strittmatter, W.S., Grain, B.J., Hulette, C.M., Joo, S.H. et al. 1993. Increased amyloid beta-peptide deposition in cerebral cortex as a consequence of apoliprotein E genotype in late-onset Alzheimer's disease. *Proc. Natl. Acad. Sci.* USA **90:**9646–9653

Selkoe, D.L. 1991. The molecular pathology of Alzheimer's disease. *Neuron* **6:**487–498

Selkoe, D.L. 1994. Alzheimer's disease: a central role for amyloid. *J. Neuropath. Exp.* Neurol. **53:**438–447

Simmons, M.A., Schneider, C.R. 1993. Amyloid β peptides act directly on single neurons. *Neurosci. Letts.* **150:**133–136

Soto, C., Kindy, M.S., Baumann, M., Frangione, B. 1996. Inhibition of Alzheimer's amyloidosis by peptides that prevent β-sheet conformation. *Biochem. Biophys. Res. Comm.* **226:**672–680

Soto, C., Sigurdsson, E.M., Morelli, L., Kumar, R.A., Castano, E.M., Frangione, B. 1998. Beta-sheet breaker peptides inhibit fibrillogenesis in a rat brain model of amyloidosis: implications for Alzheimer's therapy. *Nat. Med.* **4:**822–826

Soto, C., Saborio, G.P., Permanne, B. 2000. Inhibiting the conversion of soluble amyloid-beta peptide into abnormally folded amyloidogenic intermediates: relevance for Alzheimer's disease therapy. *Acta Neurol. Scand. Suppl.* **176:**90–95

Soto, C. 1999a. Plaque busters: strategies to inhibit amyloid formation in Alzheimer's disease. *Mol Med Today.* **5:**343–350

Soto, C. 1999b. Alzheimer's and prion disease as disorders of protein conformation: implications for the design of novel therapeutic approaches. *J. Mol. Med.* **77:**412–418

Soto, C. 2001. Protein misfolding and disease; protein refolding and therapy. *FEBS Lett*. **498:**204–207

Terzi, E., Holzemann, G., Seelig, J. 1995. Self-association of beta-amyloid peptide (1–40) in solution and binding to lipid membranes. *J. Mol Biol*. **252:**633–642

Tjernberg, L.O., Näslund, J., Lindqvist, F., Johansson, J., Karlström, A.R., Thyberg, J., Terenius, L., Nordstedt, C. 1996. Arrest of β-amyloid fibril formation by a pentapeptide ligand. *J. Biol. Chem*. **271:**8545–8548

Vargas, J., Alarcon, J.M., Rojas, E. 2000. Displacement currents associated with the insertion of Alzheimer disease amyloid β-peptide into planar bilayer membranes. *Biophys. J*. **79:**934–944

Wood, S.J., MacKenzie, L., Maleeff, B., Hurle, M.R., Wetzel, R. 1996. Selective inhibition of Abeta fibril formation. *J. Biol Chem*. **271:**4086–4092

Wood, S.J., Wetzel, R., Martin, J.D., Hurle, M.R. 1995. Prolines and amyloidogenicity in fragments of the Alzheimer's peptide beta/A4. *Biochemistry*. **34:**724–730

Yankner, B.L., Duffy, L.K., Kirschner, D.A. 1990a. Neurotropic and neurotoxic effects of amyloid beta protein: reversal by tachykinin neuropeptides. *Science* **250:**279–282

Zhu, Y.J., Lin, H., Lal, R. 2000. Fresh and nonfibrillar amyloid β protein(l–40) induces rapid cellular degeneration in aged human fibroblasts: evidence for AβP-channel-mediated cellular toxicity. *FASEB J*. **14:**1244–1254